An Automated Blood Vessel Extraction Algorithm in Fundus Images

Marwan D. Saleh, and C. Eswaran

Centre for Visual Computing,
Faculty of Computing and Informatics, Multimedia University,
Jalan Multimedia, 63100 Cyberjaya, Selangor, Malaysia
E-mail: [*marwan, eswaran*]*@mmu.edu.my*

Abstract-- This paper focuses on the extraction of retinal blood vessels which play vital roles in early diagnosis and prevention of several diseases, such as hypertension, diabetes, arteriosclerosis, cardiovascular disease and stroke. The proposed algorithm takes advantage of powerful image processing techniques such as, contrast enhancement, filtration and thresholding for more efficient segmentation. To evaluate the performance of the proposed algorithm, experiments are conducted on 40 images collected from DRIVE database. The results show that the proposed algorithm yields better results compared to other known algorithms.

Keywords: Diabetic Retinopathy; Blood vessel segmentation; Contrast enhancement; H-maxima transform; Multilevel thresholding; Wiener filter.

I. Introduction

THE interest in designing techniques for computer-aided medical diagnosis has been increasing considerably due to the rapid development in computing technology and computer industry fields. Retinal vasculature has received attention by specialists in different pathologies, where the detection and analysis of retinal vasculature may lead to early diagnosis and prevention of several diseases, such as hypertension, diabetes, arteriosclerosis, cardiovascular disease and stroke [1]. Diabetic Retinopathy (DR) is one of the well-known and the most common diseases that needs a computer-aided medical diagnosis [2]. The accurate diagnosis of this disease depends on several retinal features which have to be analyzed in order to quantify the severity level of the disease. Retinal blood vessels are considered as one of the most important features for the detection of DR. As DR is a progressive disease, regular screening of the human retina is essential for reducing the severity of the disease. The screening should be done every six months, which includes obtaining and analyzing a sequence of fundus images and observing the early changes in blood vessel patterns and the presence of other features such as microaneurysms [3-6].

In the literature, a number of algorithms for automated blood vessel segmentation have been reported. These algorithms fall into several categories, such as matched filter based [7-8], tracking based [9-12], threshold probing based [13], model based [14-15], neural network based [16], and pattern recognition based [17-18].

This paper presents an automated algorithm for the detection and extraction of blood vessels in human retina from the fundus images. The proposed algorithm takes advantage of simple and powerful image processing techniques. For instance, as the fundus images are poorly contrasted, an effective combination of top- and bottom-hat transforms [19] is utilized for contrast enhancement. Other techniques such as h-maxima transform [19] and multilevel thresholding [20] are exploited to decrease the number of intensity levels as much as possible, for making the subsequent threshold selection easier.

The rest of the paper is organized as follows: Section 2 presents an overview of the proposed algorithm, Section 3 presents the results and discussion and Section 4 provides conclusions.

II. Proposed Methodology

The proposed algorithm is designed for retinal blood vessels segmentation. Input to the system is a color fundus image of human retina acquired by a fundus camera and the output is a binary image which contains only the blood vessels. The main stages of the algorithm are: pre-processing, h-maxima transformation, multilevel thresholding, and binarization and post filtration. Fig.1 shows the block diagram of the proposed algorithm.

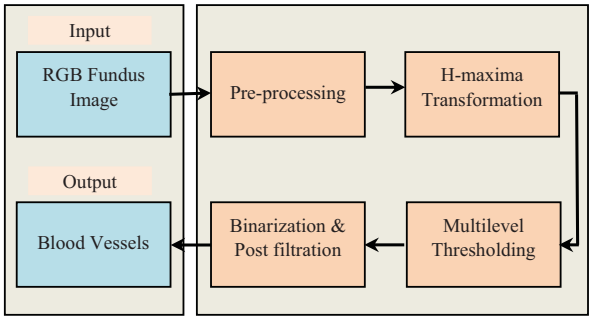

Figure 1: Block diagram of the proposed algorithm.

A. Pre-processing

Image quality varies according to the conditions of acquisition. For instance, the image could be acquired under some undesired conditions, such as unevenly illuminated or low contrasted conditions, which obviously influence the

performance of the blood vessel segmentation algorithm. Hence the acquired image has to undergo the pre-processing stage in order to improve the performance of the segmentation algorithm. The preprocessing stage comprises four steps which are: RGB to gray-scale conversion, contrast enhancement, background normalization, and filtration.

1) RGB to Gray-scale Conversion

In the first step of the pre-processing stage, RGB image is converted to gray-scale, as the gray-scale image gives a good contrast between the blood vessels and the background than the RGB image (Fig.2). Besides, the conversion to gray-scale image will decrease the computational time and also the storage space. The conversion from the colour image to gray-scale image is done by forming a weighted sum of the RGB components, as in Eq. (1)

$$g = 0.229 * R + 0.587 * G + 0.144 * B \quad (1)$$

where R, G, and B represent the red, green, and blue components respectively.

2) Contrast Enhancement

As the fundus images are poorly contrasted, it is necessary to deepen the contrast of these images to provide a better transform representation for subsequent image analysis steps [21]. In the proposed algorithm, both morphological top-hat and bottom-hat transforms are exploited to perform the contrast enhancement. In the proposed algorithm, a combination of top- and bottom-hat transforms is used for giving prominence to the blood vessels with minimal effect on the background intensity levels. Generally, the effect of the top- and bottom-hat operations are based on a predefined neighborhood or structuring element *SE*. Using a 3×3 flat *SE*, the proposed algorithm enhances the contrast of the image based on the following formula:

$$f = [(g + (g - (g \circ SE)))] - [(g \bullet SE) - g] \quad (2)$$

where f represents the contrast-enhanced gray-scale image. The result of using the combination of top- and bottom-hat transformations is shown in Fig. 2(c).

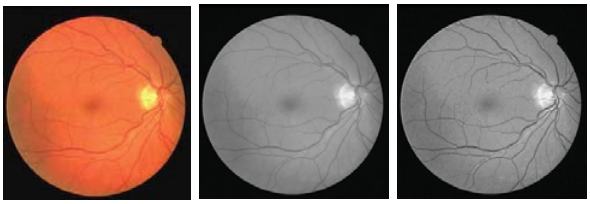

(a) (b) (c)

Figure 2: (a) original RGB image (b) Gray-scale image (c) Contrast-enhanced image

3) Background Removal

The step aims at eliminating background variations in illumination from an image so that the foreground objects may be more easily analyzed, which will represent the brighter part in the image. In the proposed algorithm, the background is removed by subtracting the contrast-enhanced image f from the median-filtered image f_{med} with a 25×25 flat *SE*, as in Eq. (3).

$$\hat{f} = f_{med} - f \quad (3)$$

The resulting image is shown in Fig. 3(b). Basically, the median filter replaces the value of a pixel (x, y) by the median of all the pixels in the neighborhood of this pixel, as in Eq. (4).

$$f_{med}(x, y) = \underset{(s,t) \in W_{xy}}{\text{median}}\{f(s,t)\} \quad (4)$$

where W represents a neighborhood centered around location (x, y) in the image. As the resulting image is low contrasted, contrast stretching is then used to obtain an image S by expanding the range of intensity values of so that the full dynamic range of the image is covered, as can be seen in Fig. 3(c).

4) Filtration

Wiener filter or *minimum mean square error* filter [22] is used for reducing the noise in the resulting image *S*. Wiener filter is a linear filter used in various digital imaging processes for enhancing images degraded by additive noise and blurring without degradation of image sharpness and colour quality, as illustrated in Fig. 3(d). The filter can be calculated as follows [23-24]:

$$W(u,v) = \frac{H^*(u,v) P_S(u,v)}{|H(u,v)|^2 + P_\eta(u,v) / P_S(u,v)} \quad (5)$$

Where:

$H(u, v)$: degradation function

$H^*(u, v)$: complex conjugate of $H(u, v)$

$|H(u, v)|2$: $H(u, v)\ H^*(u, v)$

$P_S(u, v)$: power spectrum of the undegraded image

$P_\eta(u, v)$: power spectrum of the noise

B. H-maxima Transformation

In this stage, the resulting image from the pre-processing stage is processed by the h-maxima transform [19] for reducing the number of intensity levels, which will be helpful in the subsequent stages. Let I be an intensity image; then the h-maxima transform is used for suppressing all maxima in the intensity image I whose values are less than a certain threshold h, as follows:

$$H_h(I) = R_I^\delta (I - h) \quad (6)$$

where R_I^δ describes the morphological reconstruction by dilation of image I. In general, images vary in the quality depending on the acquiring conditions. The image could be

acquired under some undesired conditions, such as unevenly distributed gray intensities, which increases the difficulty of choosing a threshold value h. By trial and error, we found that *h* can be selected based on the standard deviation value of *I*, as in Eq. (7).

$$h = \frac{2}{N \times M} \sqrt{\sum_{i=1}^{N \times M} (I_i - \mu_I)^2} \qquad (7)$$

where $N \times M$, μ denote the size, and mean value of image *I* respectively. Fig. 4(a) shows the resulting image after applying h-maxima transform to Fig. 3(d).

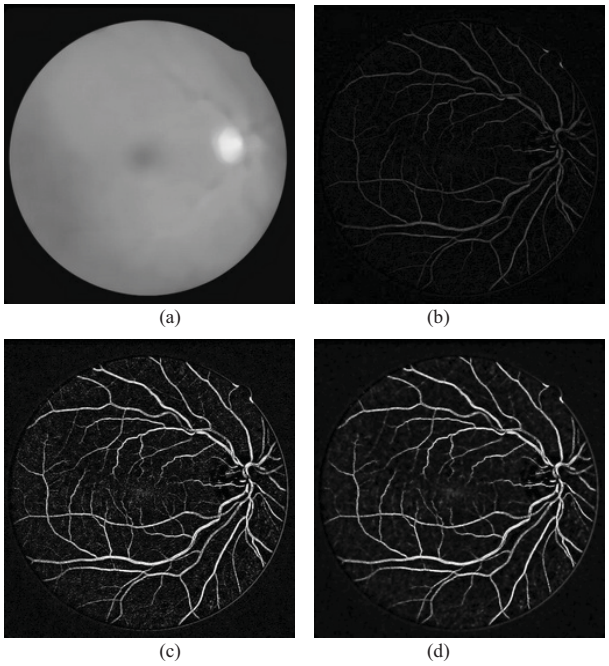

(a) (b) (c) (d)

Figure 3: (a) median-filtered image (b) removed-background image (c) contrast-stretched image (d) Wiener-filtered image using 3×3 local neighborhood

C. Multilevel Thresholding

Thresholding is one of the most commonly used techniques of image segmentation, which will highly influence the result of the algorithm. Multilevel thresholding [20] is an important technique, which converts the gray-scale image to an indexed image by decreasing the number of intensity levels so that the threshold value can be selected easily. The basic idea of this technique is to separate the pixels of an intensity image into *N* groups $G_1 \ldots G_N$, based on a certain number of threshold values T_i, as follows [25]:

$$T_i = \frac{i}{N-1}, \frac{i+1}{N-1}, \ldots, \frac{N-2}{N-1} \qquad i = 1, \ldots, N-1 \qquad (8)$$

Threshold values T_i can be obtained by analyzing the image histogram. Let *S* denotes an intensity image; then each pixel (x, y) said to be belongs to G_i if $T_{i-1} < S(x, y) \leq T_i$. In our implementation, the gray- scale levels are decreased to 4 levels to produce an image H_T in which the threshold value for binarization can be selected easily.

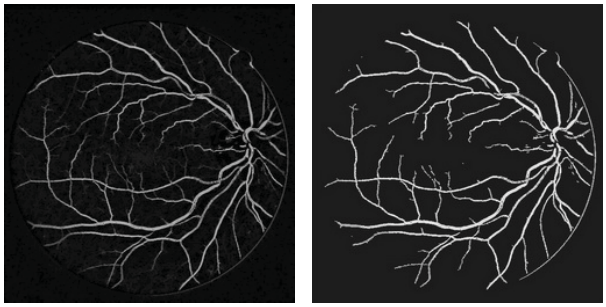

(a) (b)

Figure 4: (a) H-maxima-transformed image (b) Indexed image contains only four levels

D. Binarization and Post Filtration

The aim of this stage is to produce a binary image in which the value of each pixel is either 1(blood vessel) or 0 (background). Based on the histogram of Fig. 4(b), it can be concluded that the threshold value *T* used for binarization can be selected in the range 30 – 180, (e.g. $T = 100$). Based on the threshold value *T*, a binary image BW_1 is then obtained by thresholding the indexed image H_T, as follows:

$$BW_1(x,y) = \begin{cases} 1 & if\ H_T(x, y) \geq T \\ 0 & Otherwise \end{cases} \qquad (9)$$

As a result of the binarization, As a result of the thresholding, some unwanted pixels would appear as noise (false positive) in the resulting binary image. Therefore, some post-processing [26] is adopted for obtaining an image BW_2 by refining the image $BW_1$and retaining the desired objects.

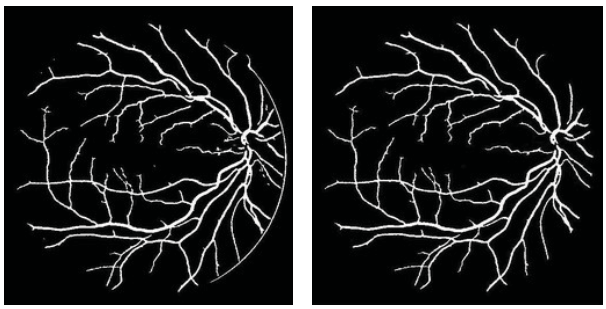

(a) (c)

Figure 5: (a) Binary image BW_1 (b) Binary image BW_2 which contains only blood vessels

III. Results and Discussion

The experiments are carried out using the same values for all

TABLE I

COMPARISON ON BLOOD VESSEL SEGMENTATION ALGORITHMS BASED ON DRIVE DATABASE

Method	*Acc.*	*TPF*	*FPF*	A_z	*k*
2nd Human observer [27]	0.9473	0.7761	0.0275	-	0.7589
Mendonca (gray-scale) [28]	0.9463	0.7315	0.0219	-	-
Mendonca (green-channel)[28]	0.9452	0.7344	0.0236	-	-
Staal [27][32]	0.9442	0.7194	0.0227	-	0.7345
Niemeijer [27][33]	0.9417	0.6898	0.0304	-	0.7145
RGB-Q [34]	-	0.7704	0.0693	-	-
G-Q [34]	-	0.7500	0.0732	-	-
Proposed Algorithm	0.9653	0.8431	0.0283	0.9281	0.7661

of the parameters mentioned in the different steps of the proposed algorithm. The performance was evaluated using sets of fundus images collected from publicly available database, called DRIVE database [27]. The DRIVE database contains 40 test images, compressed in JPEG format of size 565×584 pixels obtained from a diabetic retinopathy screening program. The images are acquired using a Canon CR5 non-mydriatic 3CCd camera at 45˚ field of view (FOV). The 40 images were divided into two sets, a test set and a training set, each containing 20 images. The images have been manually segmented by three observers to be used as references for comparing the computer generated segmentations. For each image in test set, two manual segmentations (first and second manuals) are available, whereas for an image in the training set, only one manual segmentation is available. A number of criteria, namely, accuracy (*Acc*.) [28], true positive fraction (*TPF*), false positive fraction (*FPF*) [29], area under the ROC curve (A_z) [29], and Kappa statistics (*k*) [31]. The accuracy is computed by the ratio of the total number of correctly classified points to the number of points in the image. True Positive (*TP*) refers to positive pixels correctly labeled as positive. False Positive (*FP*) refers to negative pixels incorrectly labeled as positive. False Negative (*FN*) refers to positive pixels incorrectly labeled as negative. Finally, True Negative (*TN*) refers to negative pixels correctly labeled as negative. Based on *TP*, *FP*, *FN*, and *TN*, the *TPF* and *FPF* values can be calculated using Eqns. (10) and (11) respectively.

$$TPF = \frac{TP}{TP + FN} \tag{10}$$

$$FPF = \frac{FP}{FP + TN} \tag{11}$$

where *TPF* denotes the fraction of pixels correctly classified as blood vessel pixels, while *FPF* denotes the fraction of pixels erroneously classified as blood vessel pixels.

Area under the ROC curve is obtained by plotting the True Positive Fraction (*TP*) against the False Positive Fraction (*FP*) [29]. The Kappa coefficient (*k*) is used to estimate the agreement between the automated-and manually segmented blood vessels which is calculated using Eq. (12) [31].

$$k = \frac{\Pr(a) - \Pr(e)}{1 - \Pr(e)} \tag{12}$$

where Pr(*a*) and Pr(*e*) represent the observed and chance agreements respectively. The average values of the *Acc*., *TPF*, *FPF*, A_z and *k* are obtained for the proposed algorithm using DRIVE database images. Table I compares the results obtained using the proposed algorithm with those obtained by other known algorithms

Based on the experimental results presented in Table I, it is clear that the proposed algorithm yields superior results compared to other known algorithms with respect to the accuracy and *TPF* values. The *FPF* values obtained by the proposed algorithm are comparable to the values obtained by other methods.

Based on the experimental results presented in Table I, it is clear that the proposed algorithm yields superior results compared to other known algorithms with respect to the accuracy and *TPF* values. The *FPF* values obtained by the proposed algorithm are comparable to the values obtained by other methods.

IV. CONCLUSIONS

In this paper, an efficient algorithm for retinal blood vessel segmentation has been presented. The proposed algorithm has employed techniques, such as background removal, contrast enhancement, h-maxima transformation, thresholding, etc. After converting the RGB image to gray-scale, both morphological top- and bottom-hat transforms have been exploited to perform the contrast enhancement. Other techniques such as h-maxima transform and multilevel thresholding have been exploited to decrease the intensity levels as much as possible to facilitate the threshold selection for binarization. The performance of the proposed algorithm

has been tested using DRIVE database images. From the experimental results, it is found that the proposed algorithm yields superior results compared to other known algorithms.

V. Acknowledgment

This research work is supported by E-Science Project (No: 01-02-01-SF0025) sponsored by Ministry of Science, Technology and Innovation (MOSTI), Malaysia.

VI. References

[1] J. J. Kanski, Clinical Ophthalmology: A Systematic Approach. London, U.K.: Butterworth-Heinemann, 1989.

[2] E. J. Sussman, W. G. Tsiaras, and K. A. Soper, "Diagnosis of diabetic eye disease," J. Am. Med. Assoc., vol. 247, pp. 3231–3234, 1982.

[3] S. J. Lee, C. A. McCarty, H. R. Taylor, and J. E. Keeffe, "Costs of mobile screening for diabetic retinopathy: A practical framework for rural populations," Aust. J. Rural Health, vol. 8, pp. 186–192, 2001.

[4] H. R. Taylor and J. E. Keeffe, "World blindness: A 21st century perspective," Brit. J. Ophthalmol., vol. 85, pp. 261–266, 2001.

[5] L. Streeter and M. J. Cree, "Microaneurysm detection in colour fundus images," in Image Vision Comput. New Zealand, Palmerston North, New Zealand, Nov. 2003, pp. 280–284.

[6] JVB Soares, JJG Leandro, Jr. RM Cesar, HF Jelinek, and MJ Cree. Retinal vessel segmentation using the 2-D Gabor wavelet and supervised classification. IEEE Transactions on Medical Imaging, 25(9):1214-1222, 2006.

[7] A. Hoover, V. Kouznetsova, M. Goldbaum; "Locating Blood Vessels in Retinal Images by Piecewise Threshold Probing of a Matched Filter Response", IEEE Transactions on Medical Imaging, Vol. 19, No. 3, March 2000.

[8] S. Chaudhuri, S. Chatterjee, N. Katz, M. Nelson, and M. Goldbaum, "Detection of blood vessels in retinal images using two-dimensional matched filters," IEEE Trans. Med. Imag., vol. 8, pp. 263–269, Sept. 1989.

[9] Y. Tolias and S. Panas, "A fuzzy vessel tracking algorithm for retinal images based on fuzzy clustering," IEEE Trans. Med. Imag., vol. 17, pp. 263–273, Apr. 1998.

[10] Y. Sun, "Automated identification of vessel contours in coronary arteriograms by an adaptive tracking algorithm," IEEE Trans. Med. Imag., vol. 8, pp. 78–88, Mar. 1989.

[11] S. Tamura, Y. Okamoto, and K. Yanashima, "Zero-crossing interval correction in tracing eye-fundus blood vessels," Pattern Recognit., vol. 21, no. 3, pp. 227–233, 1988.

[12] S. Tamura, K. Tanaka, S. Ohmori, K. Okazaki, A. Okada, and M. Hoshi, "Semiautomatic leakage analyzing system for time series fluorescein ocular fundus angiography," Pattern Recognit., vol. 16, no. 2, pp. 149–162, 1983.

[13] X. Jiang, D. Mojon; "Adaptive Local Thresholding by Verification-Based Multithreshold Probing with Application to Vessel Detection in Retinal Images", IEEE Transactions on Pattern Analysis and Machine Intelligence, Vol. 25, No. 1, January 2003

[14] B. D. Thackray and A. C. Nelson, "Semi-automatic segmentation of vascular network images using a rotating structuring element (ROSE) with mathematical morphology and dual feature thresholding," IEEE Trans. Med. Imag., vol. 12, pp. 385–392, Sept. 1993.

[15] A. K. Klein, F. Lee, and A. Amini, "Quantitive coronary angiography with deformable spline models," IEEE Trans. Med. Imag., vol. 16, pp. 468–482, Oct. 1997.

[16] R. Nekovei and Y. Sun, "Back-propagation network and its configuration for blood vessel detection in angiograms," IEEE Trans. Neural Networks, vol. 6, pp. 64–72, Jan. 1995.

[17] B. D. Thackray and A. C. Nelson, "Semi-automatic segmentation of vascular network images using a rotating structuring element (ROSE) with mathematical morphology and dual feature thresholding," IEEE Trans. Med. Imag., vol. 12, pp. 385–392, Sept. 1993.

[18] R. T. Ritchings and A. C. F. Colchester, "Detection of abnormalities on carotid angiograms," Pattern Recogn. Lett., vol. 4, pp. 367–374, Oct. 1986.

[19] P. Soille; "Morphological Image Analysis", 2nd Edition, Springer, 2004, ISBN: 3540429883.

[20] M. Eichmann, M. Lüssi; "Efficient Multilevel Image Thresholding". Master's thesis, Hochschule für Technik Rapperswil, Switzerland, 2005.

[21] A. K. Jain; "Fundamental of digital image processing", Prentice Hall, 1989, ISBN: 0133325764.

[22] Norbert Wiener; Extrapolation, Interpolation, and Smoothing of Stationary Time Series. New York: Wiley, 1949. ISBN 0-262-73005-7.

[23] L. W. MacDonald, M. R. Luo; "Colour Image Science", John Wiley & Sons, LTD, 2002, ISBN: 0471499277

[24] R. C. Gonzalez, R. E. Woods; "Digital Image Processing", 3rd Edition, Prentice hall, 2008. ISBN: 013168728x.

[25] The MathWorks, Inc, (1994-2010). The MATLAB package, [Online]. Available: http://www.mathworks.com/

[26] M. D. Saleh, and C. Eswaran; "An Efficient Algorithm for Retinal Blood Vessel Segmentation Using H-Maxima Transform and Multilevel Thresholding", Computer Methods in Biomechanics and biomedical Engineering, 15(5): 517-525, 2012.

[27] M. Niemeijer, and B. van Ginneken, 2002 [Online]. Available: http://www.isi.uu.nl/Reseach/Databases/DRIVE/results.php

[28] A. M. Mendonca, A. Campilho; "Segmentation of Retinal Blood Vessels by Combining the Detection of Centerlines and Morphological Reconstruction", IEEE Trans. on Med. Imag., vol. 25, no. 9, pp: 1200-1213, 2006

[29] W. J. Marshall, S. K. Bangert; "Clinical Biochemistry: Metabolic and Clinical Aspects", Elsevier Health Sciences, 1995, ISBN 0443043418

[30] C. E. Metz., "Basic Principles of ROC Analysis", Semin Nucl. Med. 8(4), 283-298, 1978.

[31] J. Cohen, "A coefficient of agreement for nominal scales", Educational and Psychological Measurement. Vol.20, No.1, pp.37–46, 1960.

[32] J. Staal, M. D. Abramoff, M. Niemeijer, M. A. Viergever, and B. Van Ginneken; "Ridge-based vessel segmentation in color images of the retina", IEEE Trans. Med. Img., vol. 23, no. 4, pp. 501-509, 2004

[33] M. Niemeijer, J. Staal, B. Van Ginneken, M. Loog, and M. D. Abramoff; "Comparative study of retinal vessel segmentation methods on a new publicly available database", SPIE Med. Image, M. Fitzpatrick and M. Sonka, eds., vol. 5370, pp. 648-656, 2004

[34] A. W. Reza , C. Eswaran , S. Hati; "Diabetic Retinopathy: A Quadtree Based Blood Vessel Detection Algorithm Using RGB Components in Fundus Images", Journal of Medical Systems, v.32 n.2, p.147-155, 2008.